



eastern side of Pre-Andes zone. The periphery of many volcanoes contains a set of magnetic anomalies consisting of medium wavelength anomaly, short wavelength anomalies, and intermediate magnetic intensity zones, and the center of the volcanoes coincides with short wavelength anomalies.

#### 4-3 Mineral Potential of the Area

Of the areas for geological reconnaissance survey of this year, the areas with porphyry copper type mineral showings and have the possibility for future exploration target are the two areas of Chusmisa and Camiña. Both areas had low Cu geochemical values, and only parts of the characteristics of porphyry copper mineralization appear at creeks, and most of the geology are covered by ignimbrite and younger volcanic rocks. As the earlier stages of prospecting for blind deposits, the geologic environment should be more important than the grade. Both areas lie within the porphyry copper belt. Of the two areas, Chusmisa show only weak mineralization at the exposures and the access is not good, thus the difficulty of exploration is deemed higher. On the other hand, in Camiña although only pyritization occurs in the phyllic alteration exposure, it is noted that several Cu showings have been reported from the vicinity.

Drill holes MJC-1 and MJC-11 confirmed quartz porphyry which is the host rock of porphyry copper mineralization and brecciated intrusive rocks and igneous intrusive bodies, and also strong pyritization in the Camarones area. This pyrite dissemination zone is similar to the Pyrite shell of San Manuel-Kalamazoo model of Lowell and Guilbert (1970). As shown in the analysis map of the area (Fig. 1-4-4), the phyllic alteration zone is developed to the east of MJC-1 and to the south of MJC-11. Therefore, there is a possibility that Cu ore shell exists between the MJC-1~MJC-12 and between MJC-12~Quebrada Camarones.

Frequency analysis of airborne magnetic data indicated the existence of characteristic magnetic anomaly pattern in altered and mineralized zones. This pattern consists of sets of a relatively large medium wavelength magnetic anomaly, small short wavelength magnetic anomalies, and intermediate magnetic intensity zones. We completed a method for delineating promising areas by pattern analysis of this magnetic anomaly pattern characteristic to porphyry copper mineralization. This method was applied to the present results and the delineated areas were overlain on the metallogenic map (Fig. 1-3-4). It is believed that the delineated areas located on the porphyry copper belt would have high porphyry copper potential. It is, however, difficult to estimate the depth of the ore horizon

from the magnetic anomaly data alone. And the exploration potential of the promising area differs by the depth of the ore horizon. Therefore, it is considered that those magnetic anomaly areas located near pre-Oligocene Series, particularly those accompanied by phyllic alteration, and covered by younger geologic units.

## CHAPTER 5 CONCLUSIONS AND RECOMMENDATIONS

### 5-1 Conclusions

The following results were obtained from the third year mineral exploration survey of the Region I area consisting of geological survey, drilling survey, and re-analysis of the airborne magnetic survey data which were acquired during the earlier part of this project.

#### Geological Survey

Magnetic susceptibility was measured for the whole area, and the results were provided for the re-analysis of the airborne magnetic survey which was carried out during the year 2000. The relation between the magnetic susceptibility and the rock species and alteration was clarified. The intrusive rocks have the highest magnetic susceptibility. The susceptibility decreases by phyllic and acidic alteration, but is not affected by propylitic alteration.

The remanent magnetism and magnetic susceptibility of samples mainly collected from outcrops of the vicinity of medium wavelength airborne magnetic low anomalies were measured. The polarity of the remanent magnetism of 6 localities out of 14 is estimated to be reverse. Also as low airborne magnetic anomalies occur in areas of high surface magnetic susceptibility, it is inferred that many airborne low magnetic anomaly zones with reverse magnetic polarity exist in the survey area. Reverse magnetic polarity and high magnetic susceptibility zones with low airborne magnetic anomaly possibly indicate blind igneous intrusion or solidified magma. This naturally is the case with high airborne magnetic anomaly areas.

A total of 14 areas extracted by airborne magnetic survey analysis as having high mineral potential were surveyed geologically for verification, and also for geological reconnaissance. As a result, Chusmisa and Camiña were extracted as areas with high mineral potential because of their relatively abundant features related to porphyry copper type mineralization. In both of the above areas, the occurrence of horizontally extensive phyllic alteration, the occurrence of porphyry or granitic rocks associated with mineralization, and the occurrence

of intrusive bodies of 65 to 48Ma were confirmed. This occurrence Paleocene to Early Eocene intrusive bodies is similar to those associated with the porphyry copper deposits in northern Chile ~ Peru. Although the above geologic features were confirmed, neither stockwork quartz veins nor Cu, Mo rock geochemical anomalies were found. The pyrite dissemination in quartz porphyry of the western alteration zone in Camiña area is similar to the Pyrite shell of the San Manuel - Kalamazoo model of Lowell and Guilbert (1970).

In the area south of Chusmisa, Paleocene-Eocene (65-48Ma) porphyry copper belt and Eocene-Oligocene (43-31Ma) porphyry copper belt occur parallel with a boundary in the N-S direction. North of Chusmisa, Paleocene-Eocene porphyry copper belt is mainly developed, and the Eocene-Oligocene belt is dissected by NW-SE trending Tertiary-Quaternary volcanic rocks. In the area north of Tignamar, Miocene intrusive bodies occur and thus the possibility of the existence of Late Eocene-Early Oligocene intrusive is believed to be small. Therefore, Late Eocene-Early Oligocene porphyry copper belt could be buried beneath the Neogene-Quaternary volcanics, and possibly may not exist as in the case of north of Tignamar.

Phyllic or acidic alteration zones were confirmed in 9 areas out of the 14 surveyed. These alteration or mineralized zones occur in: the periphery or vicinity of medium wavelength airborne magnetic anomaly zones, within or vicinity of intermediate magnetic intensity zones, and the periphery or vicinity of short wavelength anomaly zones. In these cases, about half of the medium wavelength anomalies are high anomalies and the other half low anomalies, but about 70% of the short wavelength anomalies are high anomalies. It can be said that magnetic anomalies occur near alteration zones, mineralized zones, and intrusive bodies, but the reverse is not necessarily true. And magnetic anomalies (overlap of the periphery of medium wavelength magnetic anomaly and intermediate magnetic intensity zones) do not necessarily indicate the existence of alteration zones, mineralized zones, or intrusive bodies in the shallow part.

### **Drilling**

A total of 12 holes were drilled in the overlapping zones or their vicinity of intermediate airborne magnetic intensity zones and medium wavelength magnetic anomalies. Of these, 3 holes (MJC-1, 11, 12) in the Camarones area reached the pre-Early Oligocene formations which is the porphyry copper bearing horizon. MJC-1 and MJC-11 both confirmed quartz porphyritic brecciated intrusive rocks and quartz porphyry intrusive bodies, and strong pyrite mineralization. Quartz porphyry is the host rock of the Camarones Porphyry Copper



Prospect. It is highly possible that these two drill holes located porphyry copper type mineralization and alteration. MJC-12 confirmed the occurrence of quartz diorite which is believed to be the product of Early Eocene activity, and also confirmed weak pyritization.

On the other hand, the 9 holes drilled in other areas penetrated Oligocene-Miocene conglomerate or through younger units. MJC-10 in area northeast of Camiña confirmed the occurrence of pyritization and epithermal type mineralization and acidic alteration zone in Tertiary-Quaternary volcanic rocks.

The relation between the basement depth and medium wavelength airborne magnetic anomalies or short wavelength magnetic anomalies cannot be determined from the geology of the drill holes and the changes of magnetic susceptibility of cuttings. The distance from the surface distribution of the pre-Oligocene area to the drilling site is less than 1km and this short distance is believed to be the reason for engaging the pre-Oligocene Series in Camarones area.

The general trend of the magnetic susceptibility changes of the cuttings corresponds to the changes of the geology of the drill holes. Namely the susceptibility of the mafic igneous rocks are high, and the Tertiary System and Neogene-Quaternary conglomerates are higher than that of pyroclastic rocks and shallow gravel layers. Also the magnetic susceptibility of phyllic alteration zones, acidic alteration zones, and oxidized zones are relatively low and that of the propylitic alteration zones is high.

#### **Re-analysis of Airborne Magnetic Survey**

Frequency analysis of the airborne magnetic survey data revealed magnetic anomaly patterns characteristic to porphyry copper mineralized zones. This pattern consists of a relatively large medium wavelength magnetic anomaly, small short wavelength magnetic anomalies, and intermediate magnetic intensity zones.

The genesis of this magnetic anomaly pattern is considered as follows. Medium wavelength magnetic anomaly was formed by batholithic complex body, which is a product of activity precursory to porphyry copper type mineralization. While short wavelength magnetic anomalies were formed by the plutonic and hypabyssal rocks including the ore deposits, and the intermediate magnetic intensity zones expresses the hydrothermal alteration zones associated with igneous intrusive activity.



During the process of delineating promising areas using these magnetic anomaly patterns, it is necessary to consider the following. Namely, similar magnetic anomaly patterns may appear in volcanic areas; intrusive igneous bodies may lose magnetism in large-scale alteration zones and may not be extracted as short wavelength magnetic anomalies; medium wavelength magnetic anomalies may not occur because of the interaction and mutual elimination by induction magnetism and remanent magnetism, and medium wavelength magnetic anomalies may be formed by topography and conglomerate formations.

## **5-2 Recommendations for Future Survey**

Cooperative mineral exploration carried out in the Region I Area during the past three years resulted in the acquisition airborne magnetic data, geological and geochemical data, and other information which are very relevant for mineral exploration of the area. As this area is considered to be highly prospective regarding porphyry copper deposits, it is recommended that future prospecting be carried out fully utilizing these data.

It would be desirable to take note of the following points in the future work.

### **1. Survey Methods**

In this area, thick young volcanic rocks cover the surface and it is difficult to detect the mineral deposits lying under these rocks. Airborne magnetic survey and gravity survey were implemented in order to clarify many of the problems concerning the geology of the area. The potential and problems of these methods are as follows.

#### **(1) Airborne magnetic survey**

CODELCO has shown that high macroscopic correlation exists between the major porphyry copper deposits of northern Chile and transverse magnetic anomalies. This fully applies to the major porphyry copper deposits in the central to southern parts of Region I. But transverse magnetic anomalies are not clear in the northern part, and thus in the present survey investigation was not limited to transverse magnetic anomalies, but all magnetic anomalies were analyzed and examined. Frequency analysis was adopted in order to consider the relation between porphyry copper deposits and magnetic anomalies in the level of individual anomalies. The existence of magnetic anomaly patterns each consisting of a set of medium wavelength magnetic anomaly, short wavelength magnetic anomalies, and intermediate magnetic intensity zones was discovered characteristic to known porphyry copper mineralized zones. Pattern analysis was carried out for these magnetic anomaly sets,



and the results were applied to the survey area and promising zones for mineral prospecting were extracted on this basis.

Regarding the extracted promising zones, confirmation of alteration zones, mineralized zones, and of related igneous bodies will be the next step. Two-dimensional or 3-dimensional detailed modeling using airborne magnetic data is believed to be effective for determining the existence and scale of such igneous bodies. Modeling will not necessarily provide accurate information regarding the depth of these bodies and thus application of other methods (drilling, gravity, electromagnetic methods and others) is recommended.

## (2) Gravity survey

The results of gravity survey carried out during the second year are believed to be effective for understanding the geologic structure such as the thickness of ignimbrite, but since the method is expensive in terms of areal coverage, it would be necessary to limit the area of survey. Also the usefulness of magnetic data will increase significantly by carrying out joint analysis with gravity data. In the future, if gravity survey - airborne or land - can be used to cover wide area economically, this would indeed be a very effective method to apply in this area.

## 2. Porphyry Copper Belts

Regarding the porphyry copper belt in Region I, its continuity north of Queen Elizabeth Prospect was not clear because of insufficient radiometric age data. The age determination carried out during the present survey clarified the metallogenic province of this area, and it is anticipated that the newly acquired data would contribute to the delineation of promising areas.

## 3. Promising Areas

It is recommended that the following survey be carried out in the future in order to clarify the geology and mineral deposits of the promising areas extracted by the present survey.

### (1) Magnetic anomaly zones extracted by re-analysis of airborne magnetic survey.

Extract surface manifestations by satellite image analysis in the magnetic anomaly zones delineated by pattern analysis.

### (2) Mineralized and altered zones extracted by geological survey

Carry out further detailed geological and other relevant surveys in the seven areas



extracted by geological survey, namely Mocha-Soledad, La Planada, Queen Elizabeth, Tignamar, Diana, Chusmisa, and Camiña areas.

(3) Promising areas extracted by drilling survey

Carry out further drilling for blind buried porphyry copper mineralized zones inferred to occur in the Camarones area.

## **PART II DETAILED DISCUSSIONS**

## PART II DETAILED DISCUSSIONS

### CHAPTER 1 GEOLOGICAL SURVEY

#### 1-1 Acquisition of Magnetic Data of Rocks

This survey was planned in order to acquire data for re-analysis of the results of the airborne magnetic survey, which was carried out during the second year. The survey consisted of magnetic susceptibility measurement and rock sampling along the roads accessible to vehicles and obtained representative samples covering the whole survey area.

##### 1-1-1 Measurement of magnetic susceptibility

The main targets of magnetic susceptibility measurement were outcrops near the centers of airborne magnetic short-wavelength anomalies, and other outcrops were also measured as much as possible. Magnetic susceptibility meters KT-6 (range:  $1 \times 10^{-5} \sim 999 \times 10^{-3}$  SI) manufactured by GEOFYZIKA a.s. were used. Measurement was carried out at ten points within several meters square for each outcrop. Acquired data (AP-56 at the end of this volume) were used for re-analysis of the airborne magnetic survey results.

##### 1-1-2 Measurement of remanent magnetism

###### ① Oriented samples and oriented test pieces for measurement

Sampling of oriented samples were carried out mainly at 14 outcrop sites near the airborne magnetic medium-wave anomalies. "Block oriented sampling" method, consisting of marking the strike and dip directions on a plane of the rock, was used. Three oriented samples were collected at each site. Direction was measured by clino-compass. Geomagnetic declination of Region I of Chile is slightly to the east, but the value is small and correction for the declination was not made.

More than 10 oriented test pieces were made for each site from 2 to 3 collected samples. Oriented test pieces of 25mm outer diameter and 22mm length were prepared by cutting cylinders with 1-inch outer diameter. The cylinders were drawn perpendicular to the marked plane by a corer in the laboratory.

###### ② Measurement of remanent magnetism

###### (a) Instruments and methods

SSM-2A Spinner magnetometer by Schonstedt Instruments was used for the measurement



of remanent magnetism. The output values were intensity (SI unit, A/m), declination, and inclination. The orientation at sampling time was processed as the data passed through the computer. Three axes rotating demagnetizer (Ueno and Tonouchi, 1987) was used for step-wise alternating field demagnetization.

First, the initial remanent magnetic values (INIT or int) of 10 samples were measured and intensity, declination, and inclination were obtained. Two test pieces were selected (1 piece for later measurements) and they were demagnetized progressively in alternating field as test runs, and the intensity, declination, and inclination for each piece were obtained.

The step demagnetization consisted of the following 9 steps, 5mT, 10mT, 15mT, 20mT, 25mT, 30mT, 40mT, 50mT, and 60mT. Ten measurements including the initial value were made for the test run.

Alternating field demagnetization is one method of finding hard remanent magnetism and it consists of stepwise elimination of soft remanent magnetism during demagnetization process. For example, in igneous rocks, both hard remanent magnetization acquired during magmatic cooling and soft viscous remanent magnetism (rocks are magnetized in the direction of geomagnetic field during a long period of time) exist in mixed form.

The results of stepwise alternating field demagnetization are shown in the 20 figures at the end of this volume AP-58. Demagnetization field for finding only the hard magnetization direction is determined by considering the Zijderveld plots on the left figure, intensity variation during demagnetization in the center figure, and the direction variation in the right figure.

Hard magnetization is measured by demagnetizing the remaining 8 or 9 samples from each site in the above demagnetization field. Therefore, aside from test runs, 16 to 18 samples will be measured for each site including the initial value.

This method of measuring remanent magnetization is called stable end points method (Matsumoto and Ueno, 1997). There is also the least-square method, but this requires larger number of measurements (about 3.5 times).

Regarding the present samples from Region I of Chile, 30mT demagnetization field was determined, including test runs, for all samples by the stable end points method.

#### (b) Results of remanent magnetization measurements

The initial remanent magnetism values and those after 30mT demagnetization for each site are shown in AP-58. Also the mean directions and concentration of the directions are shown in numerical values in the figures. They are; mean directions (D and I), precision parameters (k), Fisher's reliability angle for 95% (Alpha), and synthetic vector value (R). Smaller the Alpha, larger the K, and R approaching 10 indicates the concentration of direction. Also Alpha circle is shown in dotted oval in Ap-58. In the Northern Hemisphere, those with negative inclination (shown in white circles) are normal magnetization, and conversely in the Southern Hemisphere, those with positive inclination (shown in black circles) are reversed magnetization.

### 1-2 Geological Reconnaissance Survey

It was clarified by airborne magnetic survey that most of the porphyry copper type mineralization occur in zones with intermediate magnetic intensity (24,475 ~ 24,525nT) at the periphery of medium wavelength anomaly zones. Thus the third-year geological reconnaissance survey was carried out in 14 areas satisfying the above conditions and with easy access in order to elucidate the relation between airborne magnetic anomalies and geology-mineralization.

The results of the survey in the above areas are reported below. Results of: K-Ar age determination, rock thin section observation, ore polished section observation, X-ray diffraction analysis, fluid inclusion measurements, ore assay, rock geochemical analysis, and field survey are attached at the end of this volume.

The threshold values for geochemical anomalies for the second year survey were adopted for the present work. Basic statistics are laid out in Table 2-1-1. Analytical values below the limit of detection were dealt as 1/2 of the limit for statistical purposes.

#### 1-2-1 Pachica area

The sampling sites of this area are shown in Figure 2-1-1, geological map in Figure 2-1-2, schematic geologic columns in Figure 2-1-3, mineral showings in Figure 2-1-4, distribution of altered minerals in Figure 2-1-5, and rock geochemical anomaly distribution in Figure 2-1-6.

The geology of this area is composed of Lower Cretaceous System, Tertiary System,

Table 2-1-1 Basic Static Value of Rock Samples in the Geological Survey Area

| <i>Pachica</i>     | Cu (ppm) | Pb (ppm) | Zn (ppm) | Mo (ppm) | As (ppm) | Sb (ppm) | Hg (ppm) | Au (ppb) | Ag (ppm) |
|--------------------|----------|----------|----------|----------|----------|----------|----------|----------|----------|
| Average            | 50       | 27       | 107      | 7        | 28       | 2        | 0.090    | 14       | 0.6      |
| Median             | 24       | 9        | 51       | 5        | 25       | 1        | 0.023    | 3        | 0.3      |
| Standard deviation | 90       | 43       | 125      | 6        | 35       | 1        | 0.155    | 37       | 0.9      |
| Minimum            | 5        | 4        | 24       | 1        | 3        | 1        | 0.005    | 3        | 0.1      |
| Maximum            | 352      | 142      | 404      | 18       | 139      | 4        | 0.555    | 142      | 3.3      |
| Number of samples  | 14       | 14       | 14       | 14       | 14       | 14       | 14       | 14       | 14       |

| <i>Chusmisa</i>    | Cu (ppm) | Pb (ppm) | Zn (ppm) | Mo (ppm) | As (ppm) | Sb (ppm) | Hg (ppm) | Au (ppb) | Ag (ppm) |
|--------------------|----------|----------|----------|----------|----------|----------|----------|----------|----------|
| Average            | 35       | 344      | 71       | 4        | 15       | 2        | 0.075    | 4        | 1.0      |
| Median             | 25       | 9        | 64       | 4        | 3        | 1        | 0.010    | 3        | 0.1      |
| Standard deviation | 40       | 1824     | 50       | 2        | 33       | 1        | 0.243    | 8        | 4.8      |
| Minimum            | 7        | 1        | 10       | 1        | 3        | 1        | 0.005    | 3        | 0.1      |
| Maximum            | 200      | 10000    | 284      | 8        | 171      | 7        | 1.199    | 48       | 26.5     |
| Number of samples  | 30       | 30       | 30       | 30       | 29       | 29       | 29       | 30       | 30       |

| <i>Chusmisa NE</i> | Cu (ppm) | Pb (ppm) | Zn (ppm) | Mo (ppm) | As (ppm) | Sb (ppm) | Hg (ppm) | Au (ppb) | Ag (ppm) |
|--------------------|----------|----------|----------|----------|----------|----------|----------|----------|----------|
| Average            | 20       | 16       | 20       | 8        | 21       | 2        | 0.427    | 3        | 0.1      |
| Median             | 12       | 14       | 15       | 3        | 7        | 1        | 0.049    | 3        | 0.1      |
| Standard deviation | 17       | 13       | 13       | 13       | 40       | 3        | 1.162    | 3        | 0.2      |
| Minimum            | 4        | 1        | 2        | 1        | 3        | 1        | 0.005    | 3        | 0.1      |
| Maximum            | 53       | 58       | 42       | 51       | 172      | 12       | 5.074    | 13       | 0.6      |
| Number of samples  | 21       | 21       | 21       | 21       | 20       | 20       | 20       | 21       | 21       |

| <i>Camiña</i>      | Cu (ppm) | Pb (ppm) | Zn (ppm) | Mo (ppm) | As (ppm) | Sb (ppm) | Hg (ppm) | Au (ppb) | Ag (ppm) |
|--------------------|----------|----------|----------|----------|----------|----------|----------|----------|----------|
| Average            | 30       | 10       | 46       | 5        | 20       | 1        | 0.010    | 3        | 0.1      |
| Median             | 26       | 7        | 48       | 4        | 10       | 1        | 0.005    | 3        | 0.1      |
| Standard deviation | 15       | 10       | 30       | 5        | 31       | 0        | 0.012    | 0        | 0.1      |
| Minimum            | 9        | 1        | 6        | 1        | 3        | 1        | 0.005    | 3        | 0.1      |
| Maximum            | 62       | 35       | 108      | 27       | 119      | 1        | 0.057    | 3        | 0.6      |
| Number of samples  | 27       | 27       | 27       | 27       | 24       | 24       | 24       | 27       | 27       |

| <i>Camiña</i>      | Cu (ppm) | Pb (ppm) | Zn (ppm) | Mo (ppm) | As (ppm) | Sb (ppm) | Hg (ppm) | Au (ppb) | Ag (ppm) |
|--------------------|----------|----------|----------|----------|----------|----------|----------|----------|----------|
| Average            | 4598     | 15       | 59       | 2        | 68       | 2        | 0.011    | 4        | 0.2      |
| Median             | 75       | 8        | 52       | 1        | 40       | 1        | 0.008    | 3        | 0.1      |
| Standard deviation | 15001    | 29       | 30       | 2        | 75       | 1        | 0.008    | 5        | 0.5      |
| Minimum            | 10       | 1        | 25       | 1        | 3        | 1        | 0.005    | 3        | 0.1      |
| Maximum            | 60392    | 138      | 162      | 6        | 254      | 6        | 0.029    | 24       | 2.2      |
| Number of samples  | 22       | 22       | 22       | 22       | 20       | 20       | 20       | 22       | 22       |

| <i>Camiña NE</i>   | Cu (ppm) | Pb (ppm) | Zn (ppm) | Mo (ppm) | As (ppm) | Sb (ppm) | Hg (ppm) | Au (ppb) | Ag (ppm) |
|--------------------|----------|----------|----------|----------|----------|----------|----------|----------|----------|
| Average            | 20       | 13       | 7        | 5        | 54       | 1        | 0.027    | 3        | 0.1      |
| Median             | 20       | 13       | 7        | 5        | 54       | 1        | 0.027    | 3        | 0.1      |
| Standard deviation | 22       | 6        | 6        | 3        | 72       | 0        | 0.012    | 0        | 0.0      |
| Minimum            | 4        | 8        | 2        | 3        | 3        | 1        | 0.018    | 3        | 0.1      |
| Maximum            | 35       | 17       | 11       | 7        | 105      | 1        | 0.035    | 3        | 0.1      |
| Number of samples  | 2        | 2        | 2        | 2        | 2        | 2        | 2        | 2        | 2        |

| <i>Tigamar NW</i>  | Cu (ppm) | Pb (ppm) | Zn (ppm) | Mo (ppm) | As (ppm) | Sb (ppm) | Hg (ppm) | Au (ppb) | Ag (ppm) |
|--------------------|----------|----------|----------|----------|----------|----------|----------|----------|----------|
| Average            | 47       | 1700     | 54       | 3        | 1403     | 2        | 0.075    | 3        | 0.2      |
| Median             | 46       | 45       | 38       | 2        | 30       | 1        | 0.052    | 3        | 0.2      |
| Standard deviation | 28       | 4066     | 61       | 3        | 3371     | 1        | 0.081    | 0        | 0.1      |
| Minimum            | 18       | 12       | 2        | 1        | 3        | 1        | 0.005    | 3        | 0.1      |
| Maximum            | 90       | 10000    | 171      | 8        | 8284     | 4        | 0.232    | 3        | 0.3      |
| Number of samples  | 6        | 6        | 6        | 6        | 6        | 6        | 6        | 6        | 6        |

| <i>Tigamar SE</i>  | Cu (ppm) | Pb (ppm) | Zn (ppm) | Mo (ppm) | As (ppm) | Sb (ppm) | Hg (ppm) | Au (ppb) | Ag (ppm) |
|--------------------|----------|----------|----------|----------|----------|----------|----------|----------|----------|
| Average            | 26       | 70       | 29       | 1        | 532      | 14       | 0.087    | 3        | 0.2      |
| Median             | 15       | 26       | 31       | 1        | 641      | 1        | 0.029    | 3        | 0.1      |
| Standard deviation | 25       | 86       | 19       | 0        | 484      | 23       | 0.121    | 0        | 0.1      |
| Minimum            | 8        | 15       | 10       | 1        | 3        | 1        | 0.005    | 3        | 0.1      |
| Maximum            | 54       | 170      | 47       | 1        | 951      | 40       | 0.226    | 3        | 0.3      |
| Number of samples  | 3        | 3        | 3        | 3        | 3        | 3        | 3        | 3        | 3        |

| <i>Putre S</i>     | Cu (ppm) | Pb (ppm) | Zn (ppm) | Mo (ppm) | As (ppm) | Sb (ppm) | Hg (ppm) | Au (ppb) | Ag (ppm) |
|--------------------|----------|----------|----------|----------|----------|----------|----------|----------|----------|
| Average            | 44       | 17       | 53       | 3        | 18       | 2        | 0.031    | 4        | 0.3      |
| Median             | 21       | 12       | 16       | 3        | 7        | 1        | 0.015    | 3        | 0.1      |
| Standard deviation | 58       | 15       | 74       | 2        | 24       | 1        | 0.053    | 3        | 0.8      |
| Minimum            | 6        | 1        | 5        | 1        | 3        | 1        | 0.005    | 3        | 0.1      |
| Maximum            | 230      | 62       | 293      | 6        | 87       | 3        | 0.212    | 12       | 3.2      |
| Number of samples  | 16       | 16       | 16       | 16       | 14       | 14       | 14       | 16       | 16       |

| <i>Putre W</i>     | Cu (ppm) | Pb (ppm) | Zn (ppm) | Mo (ppm) | As (ppm) | Sb (ppm) | Hg (ppm) | Au (ppb) | Ag (ppm) |
|--------------------|----------|----------|----------|----------|----------|----------|----------|----------|----------|
| Average            | 12417    | 59       | 184      | 10       | 7        | 2        | 0.016    | 32       | 3.6      |
| Median             | 2091     | 14       | 30       | 6        | 4        | 2        | 0.010    | 8        | 0.8      |
| Standard deviation | 15886    | 101      | 509      | 7        | 8        | 1        | 0.015    | 74       | 5.3      |
| Minimum            | 29       | 3        | 6        | 3        | 3        | 1        | 0.005    | 3        | 0.1      |
| Maximum            | 41170    | 378      | 2005     | 28       | 27       | 2        | 0.046    | 293      | 17.2     |
| Number of samples  | 15       | 15       | 15       | 15       | 10       | 10       | 10       | 15       | 15       |

| <i>Arica E</i>     | Cu (ppm) | Pb (ppm) | Zn (ppm) | Mo (ppm) | As (ppm) | Sb (ppm) | Hg (ppm) | Au (ppb) | Ag (ppm) |
|--------------------|----------|----------|----------|----------|----------|----------|----------|----------|----------|
| Average            | 2903     | 231      | 267      | 17       | 149      | 4        | 0.086    | 242      | 10.9     |
| Median             | 2903     | 231      | 267      | 17       | 149      | 4        | 0.086    | 242      | 10.9     |
| Standard deviation | 1803     | 45       | 122      | 18       | 57       | 4        | 0.018    | 43       | 0.2      |
| Minimum            | 1628     | 199      | 181      | 4        | 108      | 1        | 0.073    | 211      | 10.7     |
| Maximum            | 4178     | 262      | 353      | 29       | 189      | 6        | 0.099    | 272      | 11.0     |
| Number of samples  | 2        | 2        | 2        | 2        | 2        | 2        | 2        | 2        | 2        |



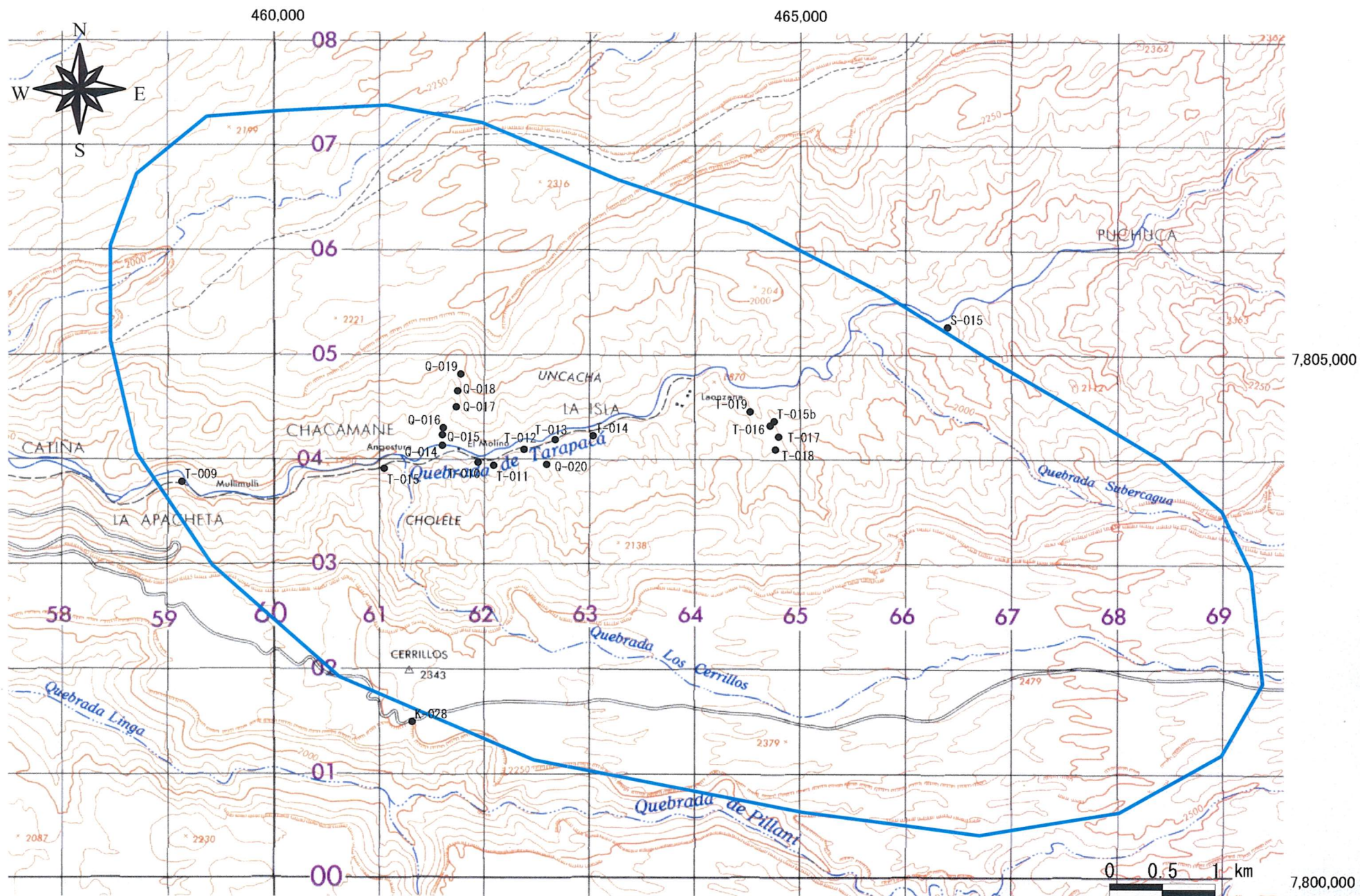


Fig. 2-1-1 Sample Location Map of the Pachica Area



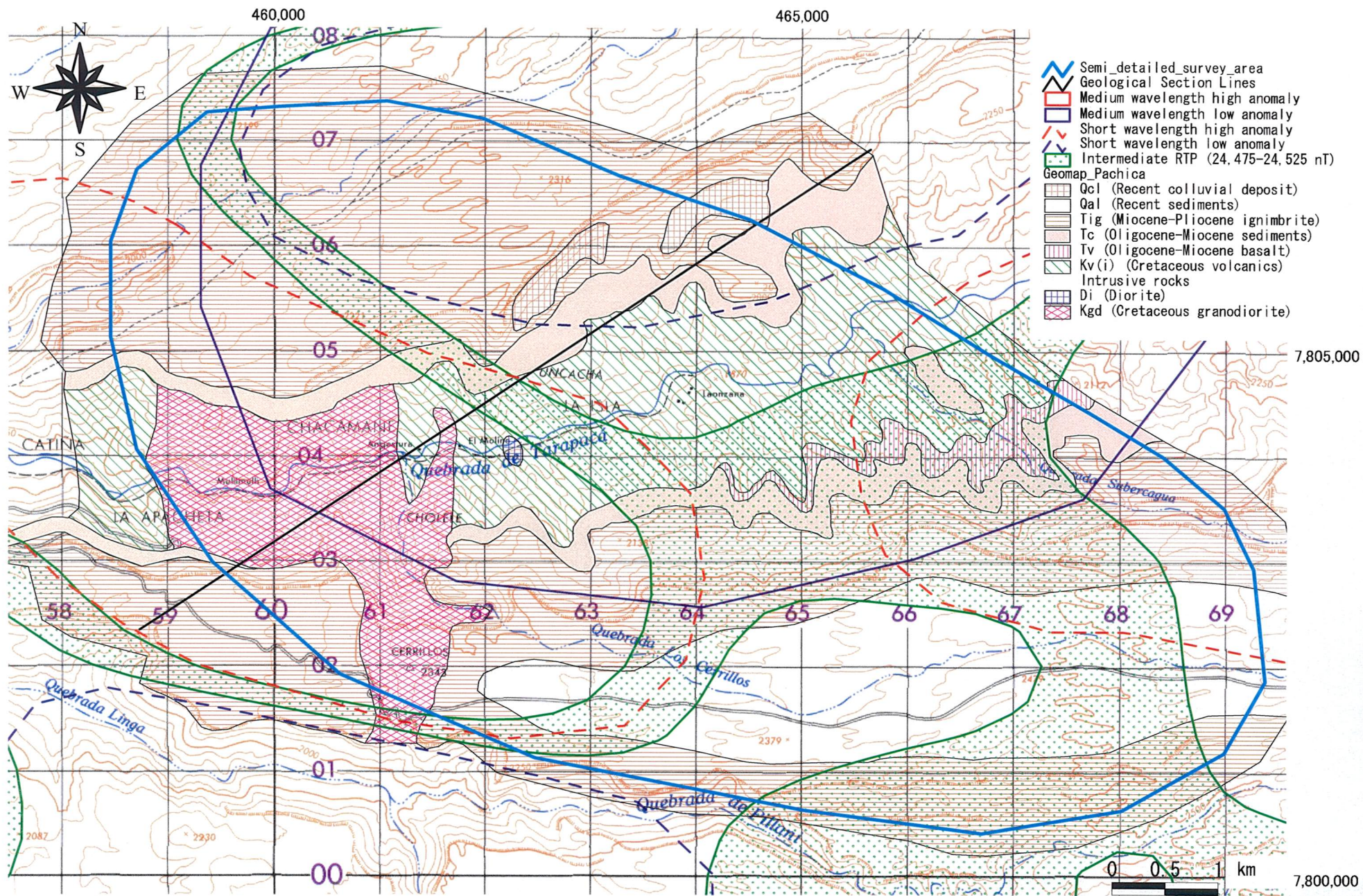
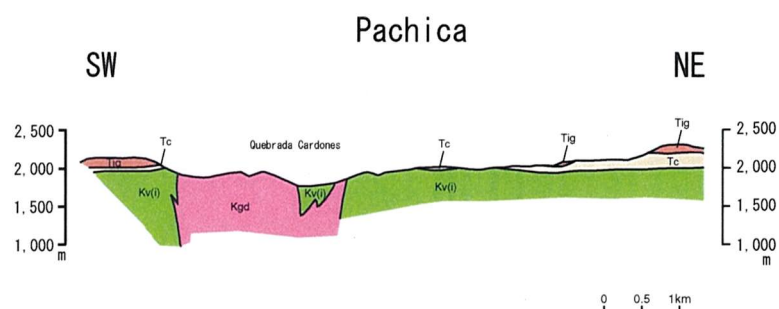


Fig. 2-1-2 Geological Map of the Pachica Area





| Geologic Time |            | Columnar Section          | Lithology                          | Intrusives                                   | Mineralization |
|---------------|------------|---------------------------|------------------------------------|--|----------------|
| CENOZOIC      | QUATERNARY | HOLOCENE                  | Talus<br>Alluvium                  | Granodiorite (Kgd)<br>↑<br>Diorite (Di)<br>↑ | pyrite, barite |
|               | TERTIARY   | PLIOCENE<br>~<br>MIOCENE  | Welded tuff<br><br>Pumice tuff     |  |                |
|               |            | MIOCENE<br>~<br>OLIGOCENE | Conglomerate<br><br>Basalt         |  |                |
|               |            | PALEOGENE                 |                                    |  |                |
| MESOZOIC      | CRETACEOUS | LATE                      |                                    |  |                |
|               | EARLY      | Kv(i) Kgd Di Kv(i)        | Andesitic lava/<br>volcaniclastics |  |                |

Fig. 2-1-3 Schematic Stratigraphic Columns and Profiles of the Pachica Area



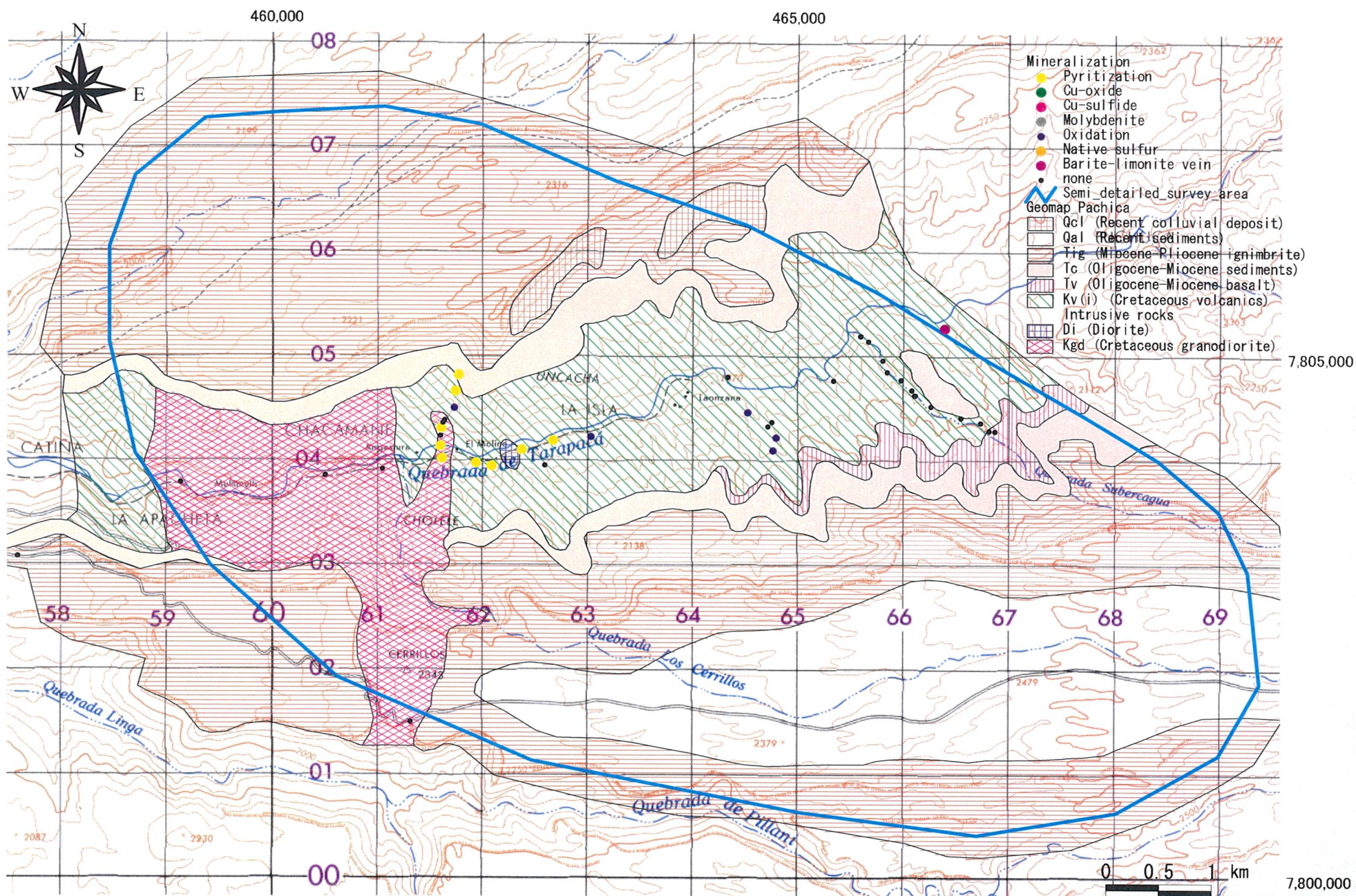
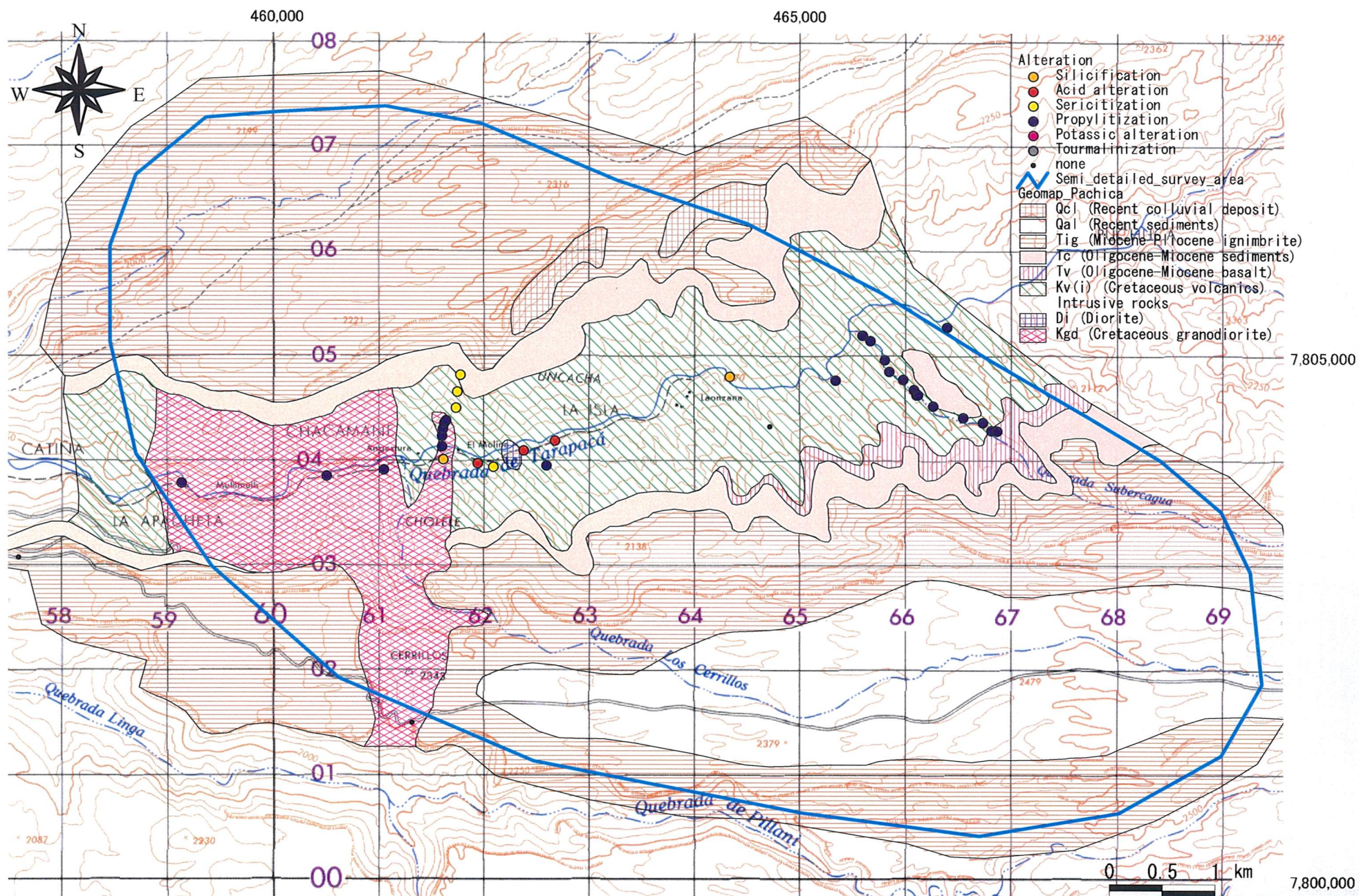


Fig. 2-1-4 Mineralization Map of the Pachica Area







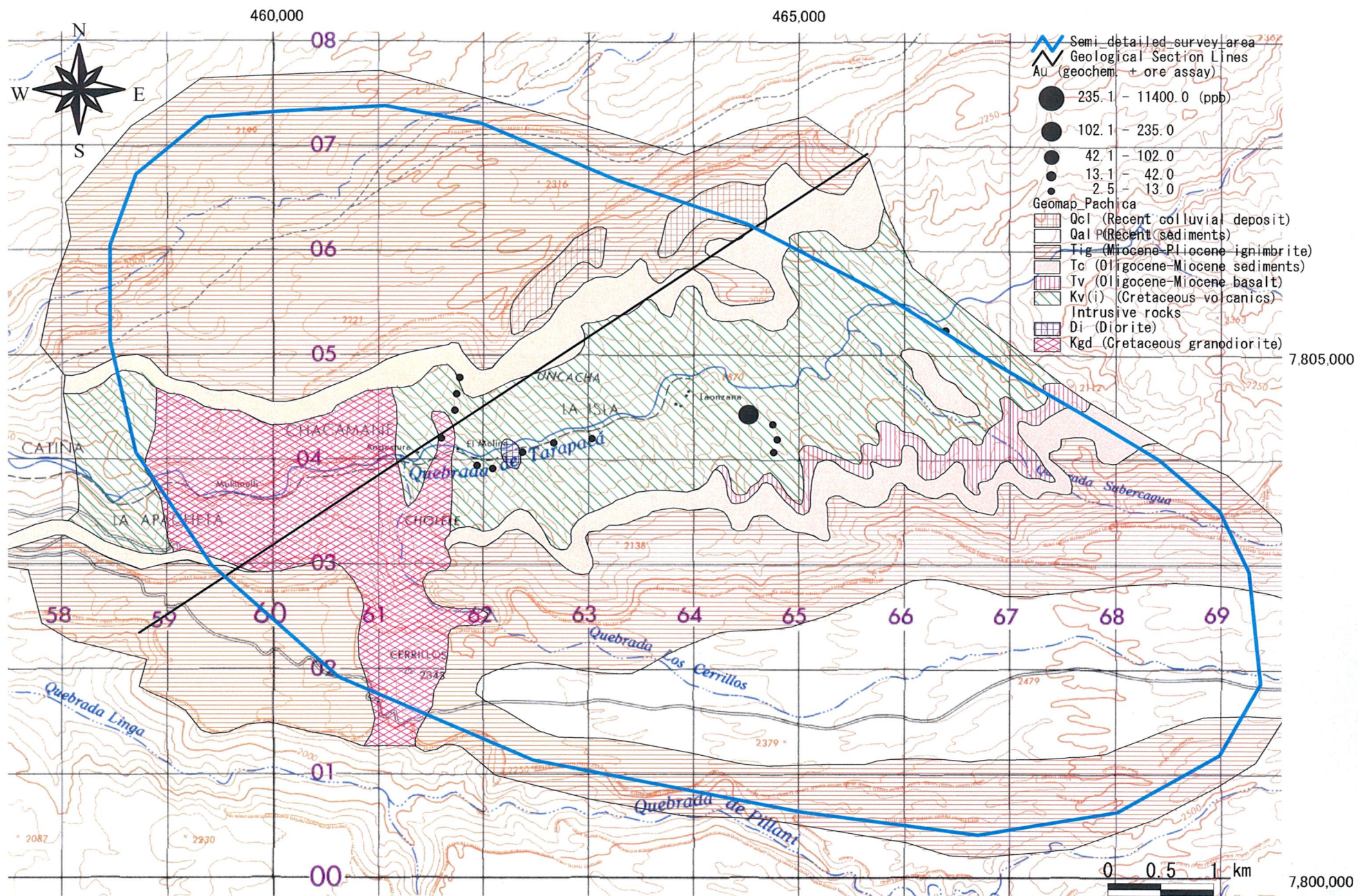


Fig. 2-1-6 (1) Geochemical Anomaly Map in the Pachica Area (Au)



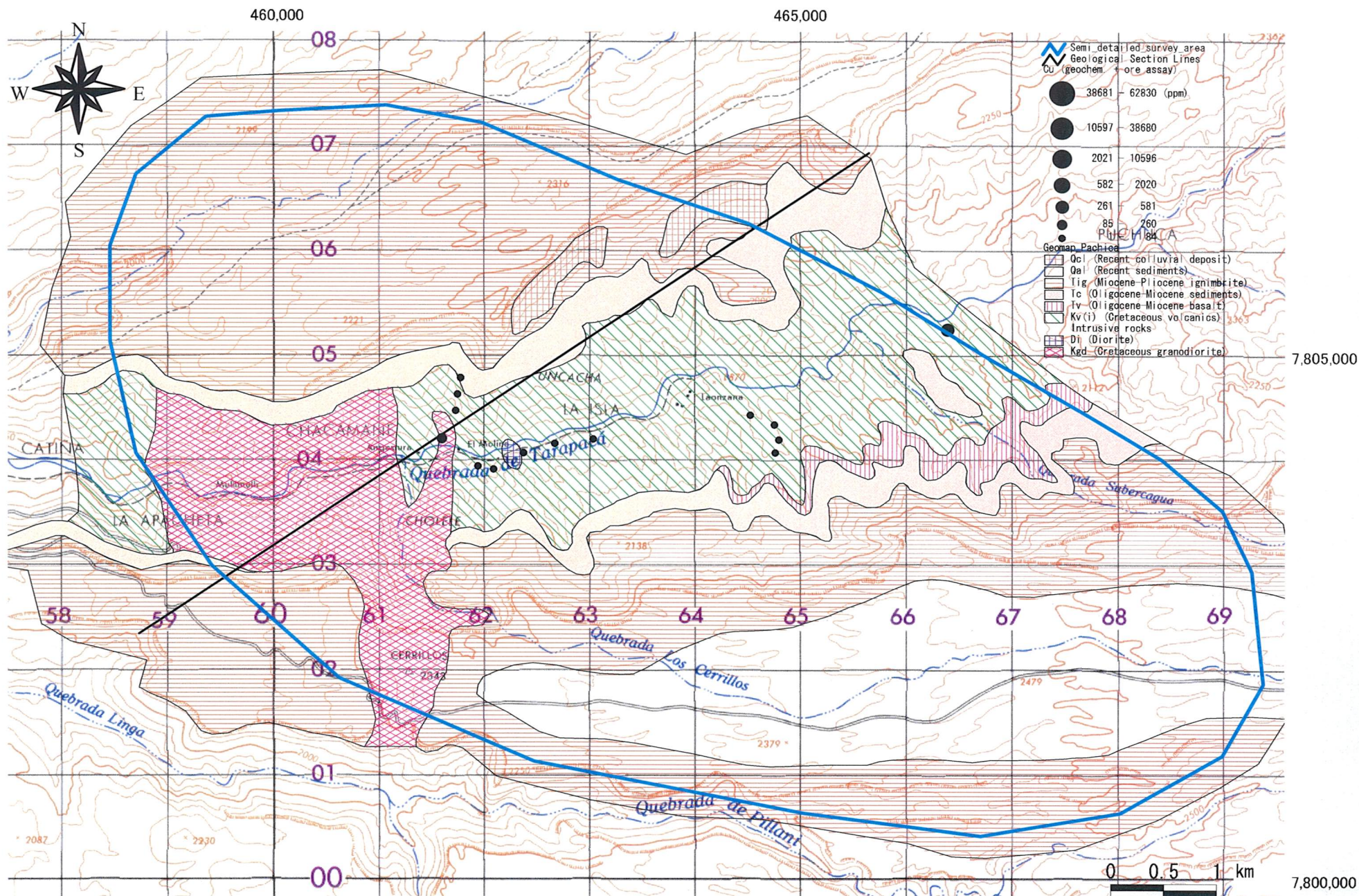


Fig. 2-1-6 (2) Geochemical Anomaly Map in the Pachica Area (Cu)



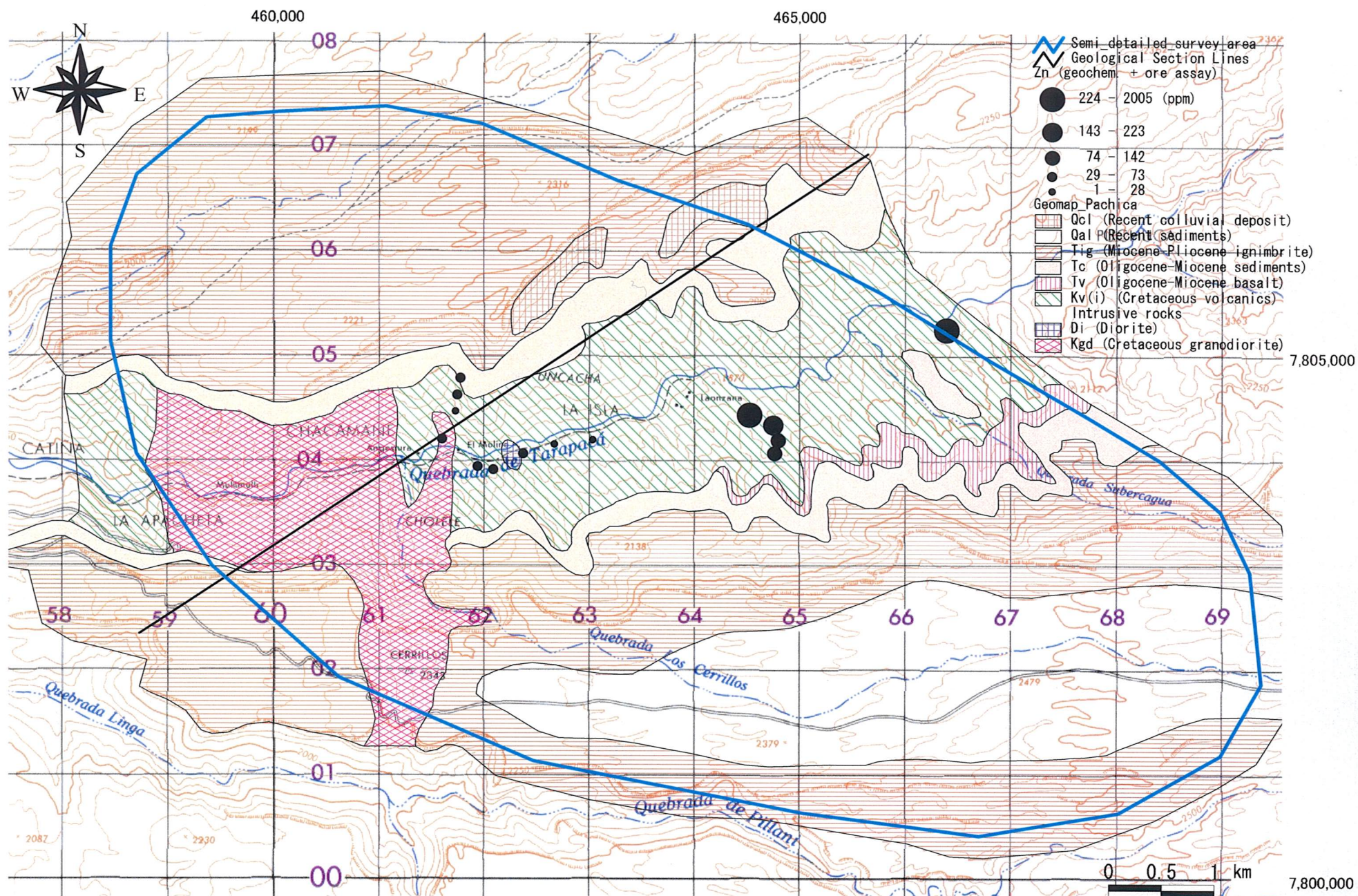


Fig. 2-1-6 (3) Geochemical Anomaly Map in the Pachica Area (Zn)